

Search for Jacobi shape transition in $A \sim 30$ nuclei

Balaram Dey,¹ C. Ghosh,¹ Deepak Pandit,² A.K. Rhine Kumar,³ S. Pal,⁴ V. Nanal,^{1,*} R.G. Pillay,¹ P. Arumugam,⁵ S. De,⁶ G. Gupta,¹ H. Krishnamoorthy,⁷ E.T. Mirgule,⁶ Surajit Pal,² and P.C. Rout⁶

¹*Department of Nuclear and Atomic Physics, Tata Institute of Fundamental Research, Mumbai-400005, India*

²*Variable Energy Cyclotron Centre, 1/AF-Bidhannagar, Kolkata-700064, India*

³*Department of Physics, Cochin University of Science and Technology, Cochin-682022, Kerala, India.*

⁴*Pelletron Linac Facility, Tata Institute of Fundamental Research, Mumbai-400005, India*

⁵*Department of Physics, Indian Institute of Technology, Roorkee-247667, India*

⁶*Nuclear Physics Division, Bhabha Atomic Research Centre, Mumbai-400085, India*

⁷*Indian Neutrino Observatory, Tata Institute of Fundamental Research and Homi Bhabha National Institute, Mumbai-400085, India*
(Dated: March 12, 2022)

This paper reports the first observation of the Jacobi shape transition in ^{31}P using high energy γ -rays from the decay of giant dipole resonance (GDR) as a probe. The measured GDR spectrum in the decay of ^{31}P shows a distinct low energy component around 10 MeV, which is a clear signature of Coriolis's splitting in a highly deformed rotating nucleus. Interestingly, a self-conjugate α -cluster nucleus ^{28}Si , populated at similar initial excitation energy and angular momentum, exhibits a vastly different GDR line shape. Even though the angular momentum of the compound nucleus ^{28}Si is higher than the critical angular momentum required for the Jacobi shape transition, the GDR lineshape is akin to a prolate deformed nucleus. Considering the present results for ^{28}Si and similar observation recently reported in ^{32}S , it is proposed that the nuclear orbiting phenomenon exhibited by α -cluster nuclei hinders the Jacobi shape transition. The present experimental results suggest a possibility to investigate the nuclear orbiting phenomenon using high energy γ -rays as a probe.

Many body quantum systems like atomic nuclei provide a unique opportunity to explore a variety of phenomena arising due to interplay of different physical processes, particularly at high excitation energy (E^*) and angular momentum (J). One such interesting phenomenon is the Jacobi shape transition, where beyond a critical angular momentum (J_C), an abrupt shape change from non-collective oblate shape to collective triaxial or prolate shape takes place [1]. The study of exotic Jacobi shapes in nuclei has been a topic of considerable interest [2, 3]. The Jacobi shape transition is expected to occur in light and medium mass nuclei, where high rotational frequencies are achieved before the excited nucleus can undergo fission. Further, it is expected that the Jacobi shape transition should be a common feature over a wide range of nuclei. Experimentally, the Jacobi shape transition has been observed in a few light mass nuclei $A \sim 45$ [4–7] via the γ -decay of giant dipole resonance (GDR). It is known that the GDR is the cleanest, and hence most extensively used, probe to study the properties of nuclei at high temperature (T) and J [8]. The GDR can be understood macroscopically as an out-of-phase oscillation between protons and neutrons, and microscopically in terms of coherent particle-hole excitations. The GDR γ -emission occurs at the early stage of compound nucleus (CN) decay and can probe the nuclear shape. The GDR components corresponding to vibration along and perpendicular to the axis of rotation are differently affected by the Coriolis's force. As a result the GDR strength function splits into multiple components with a narrow well separated peak around 8-10 MeV [4], which is an unambiguous signature of the Jacobi shape transition. It should be mentioned that the search for Jacobi shapes has also been made through studies of quasi-continuum gamma radiation [9]. However, indications of highly deformed shapes could not be uniquely ascribed to the Jacobi shape.

While many of the observed features of nuclei at high E^* , J can be understood in terms of rotating liquid drop model (RLDM) and mean field approach, it is well known that nuclei also exhibit cluster structure [10–13]. The influence of clustering in the stellar nucleosynthesis has been a long-standing question in nuclear astrophysics [14–16]. Nuclear orbiting phenomena involving formation of a long-lived dinuclear molecular complex, with a strong memory of the entrance channel, has been observed in reactions involving self conjugate α -cluster nuclei [17, 18]. Such an orbiting dinuclear system can attain complicated exotic shapes as compared to a shape equilibrated compound nucleus [10, 17, 19–21]. Interestingly, recent studies of GDR spectrum from the ^{32}S nucleus populated with $J > J_C$ in the reaction $^{20}\text{Ne} + ^{12}\text{C}$, did not show evidence of the Jacobi shape transition [7, 23] and the result was interpreted in terms of the formation of $^{16}\text{O} + ^{16}\text{O}$ molecular structure in a superdeformed state of ^{32}S . The observation of a narrow resonance in $^{24}\text{Mg} + ^{24}\text{Mg}$ at $J = 36 \hbar$ [22] was interpreted in terms of the highly deformed shape corresponding to a molecular state, but no clear signature of the Jacobi shape transition was observed.

*e-mail:nanal@tifr.res.in

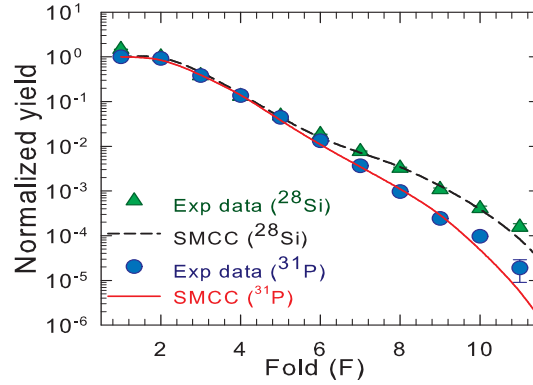


FIG. 1: (Color online) Experimental fold distribution (symbol) together with that from the SMCC calculations (line) for $^{19}\text{F}+^{12}\text{C}$ and $^{16}\text{O}+^{12}\text{C}$ reactions.

Therefore, experimental studies of the exotic shapes of different nuclei with $J > J_C$ are crucial to understand the different mechanisms like the nuclear orbiting, cluster formation and Jacobi shape transition. The aim of the present study is to investigate the deformed shapes of a α -cluster (^{28}Si) and a non- α -cluster (^{31}P) nuclei at high J using the GDR as a probe. This work also addresses the open question whether the Jacobi shape transition is a general phenomenon in light mass nuclei.

The experiments were performed using pulsed beams of ^{19}F (at $E_{\text{lab}}=127$ MeV) and ^{16}O (at $E_{\text{lab}}=125$ MeV) from the Pelletron Linac Facility (PLF), Mumbai bombarding a self-supporting ^{12}C target ($400 \mu\text{g}/\text{cm}^2$). The high energy γ -rays in the region of 5-30 MeV were measured using an array of seven close packed hexagonal BaF_2 detectors (each 20 cm long with face-to-face distance of 9 cm) mounted at 125° with respect to the beam direction and at a distance of 57 cm from the target position. A 14-element BGO multiplicity filter (hexagonal, 6.3 cm long and 5.6 cm face-to-face) was mounted in a castle geometry surrounding the target ($\sim 60\%$ efficiency at 662 keV), for measuring the multiplicity (M) of low energy discrete γ -rays to extract the angular momentum information. The BaF_2 array was surrounded by an annular plastic detector which was used as a cosmic ray veto. Detector arrays, upstream collimators and the beam dump (kept at ~ 2 m from the target) were suitably shielded to minimize the background. The anode output of individual BaF_2 detector was integrated in two different gates of width 200 ns (E_{short}) and $2 \mu\text{s}$ (E_{long}) for pileup rejection using pulse shape discrimination (PSD) and energy measurement, respectively. The time-of-flight (TOF) of each BaF_2 detector with respect to the RF pulse was used to reject neutron events. For each event E_{short} , E_{long} , BaF_2 -TOF of each BaF_2 detector were recorded together with the fold F (number of BGO detectors fired for $E_{\text{th}} > 120$ keV within a 50 ns coincidence window) and BGO-TOF with respect to the RF pulse [24]. The energy calibration of the BaF_2 detector array was obtained using low energy radioactive sources and was linearly extrapolated to high energies. The gain stability of the BaF_2 detectors was found to be within $\pm 1\%$. The beam induced background contributions were also monitored with a blank target frame and were found to be negligible. Further details of the experimental setup can be found in Ref. [25].

The high energy γ -ray spectra for different folds are generated in offline analysis after incorporating corrections due to chance coincidence and Doppler effect arising from the finite recoil velocity of the residues. The γ -ray spectra for $F \geq 4$ were analyzed within the statistical model framework using the code SMCC [26] to extract the GDR parameters, $\langle T \rangle$ and $\langle J \rangle$ following the procedure in Ref. [25]. In both systems, the data corresponding to lower folds ($F \leq 3$) were not considered as it can have contributions from radioactivity and extraneous background. The optical model parameters are taken from Ref. [27–29] and Ignatyuk level density prescription [30] is used with $\tilde{a} = A/7 \text{ MeV}^{-1}$ [31]. The effective moment of inertia is assumed to be $I_{\text{eff}} = I_0(1 + \delta_1 J^2 + \delta_2 J^4)$, where $I_0 (= \frac{2}{5} A^{5/3} r_0^2)$ is the rigid-body moment of inertia, r_0 is radius parameter, δ_1 and δ_2 are deformation parameters. The residue spin distribution (J_{res}) is calculated starting from the standard J_{CN} distribution and is converted to the multiplicity M using the relative decay probability (P_r) of dipole and quadrupole transitions as a parameter. The M distribution is then converted to the fold (F) distribution incorporating the BGO array efficiency and crosstalk probability as described in Ref. [32]. All three parameters, namely, P_r , δ_1 and δ_2 are varied to fit the experimentally observed fold distribution. The fold distributions thus calculated with the SMCC for both systems are shown in Fig. 1 together with the data. It is important to note that both reactions are studied in the same setup and with a similar analysis, to rule out any systematic factors that could affect the data.

The γ -ray spectrum in the SMCC is calculated assuming $\sim 100\%$ TRK sum rule and the GDR line shape is taken as a sum of multiple (2 to 5) Lorentzian components. A bremsstrahlung contribution is computed from systematics [33]

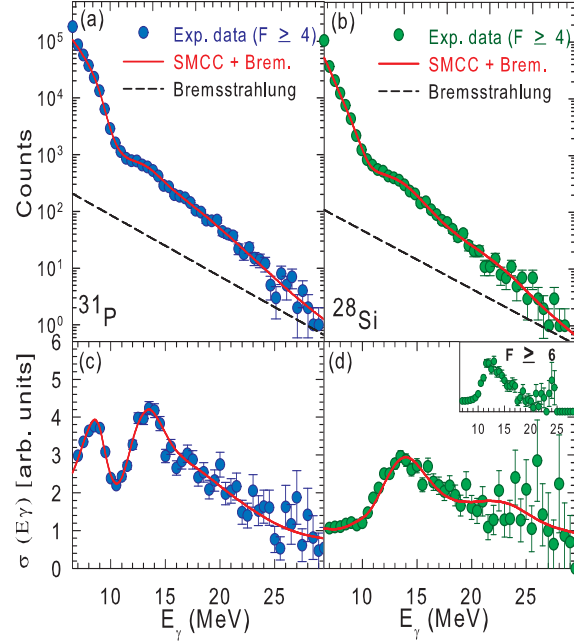


FIG. 2: (Color online) Fold gated high energy γ -ray spectra (symbols) with the best fit SMCC calculation (line) for (a) ^{31}P and (b) ^{28}Si ; corresponding divided plots are shown in panel (c) and (d). Divided plot for ^{28}Si with $F \geq 6$ is shown as an inset in panel (d).

as (e^{-E_γ/E_0}) with $E_0 = 1.1[(E_{lab} - V_c)/A_p]^{0.72}$, where E_{lab} , V_c and A_p are the beam energy, Coulomb barrier and the projectile mass, respectively. The bremsstrahlung spectrum folded with the detector response function was added to the calculated GDR spectrum for comparison with data. The goodness of the fit is achieved by χ^2 minimization and visual inspection in the energy range of $E_\gamma = 7 - 25$ MeV. Fold gated high energy γ -ray spectra and the divided plots (generated using a γ -ray spectrum calculated with an arbitrary constant dipole strength of 0.2 W.u. folded with the BaF₂ array response) together with the best fit statistical model calculations for both ^{31}P and ^{28}Si are shown in Fig. 2. The GDR spectrum of ^{31}P could be not be fitted with prolate/oblate shape (2-component Lorentzian function) or a triaxial shape (3-component Lorentzian function). The observed spectrum has five Lorentzian components, resulting from the Jacobi shape transition. To restrict the fitting window (for large no. of parameters), initial values for centroid energy (E_i), width (Γ_i) and strength (S_i) were taken from Ref. [34] and then varied individually within a limited range to achieve the best fit. In case of ^{28}Si , a two component strength function corresponding to a prolate shape describes the data well. The best fit GDR parameters for both the nuclei are given in Table I. It should be

TABLE I: Best fit GDR parameters from the SMCC analysis.

System	$\langle J \rangle (\hbar)$	$\langle T \rangle$ (MeV)	E_{GDR} (MeV)	Γ_{GDR} (MeV)	S_{GDR}
^{31}P	22(6)	2.2(3)	9.1(1)	2.2(1)	0.18(2)
			14.2(3)	4.4(2)	0.30(1)
			18.2(4)	7.3(4)	0.18(2)
			20.0(6)	8.8(5)	0.14(3)
			23.0(8)	9.6(8)	0.16(3)
^{28}Si	21(6)	2.1(3)	14.6(3)	6.0(3)	0.44(4)
			24.6(8)	10.0(7)	0.62(3)

mentioned that the GDR lineshape is not expected to be very sensitive to the level density parameter [35]. In the present case, the extracted GDR parameters corresponding to $\tilde{a} = A/7$ and $A/8$, are same within fitting errors. The effect of direct reactions like pre-equilibrium emission, incomplete fusion etc. is not considered, since it has been shown to be negligible for $^{16}\text{O}+^{12}\text{C}$ at the present beam energy [36].

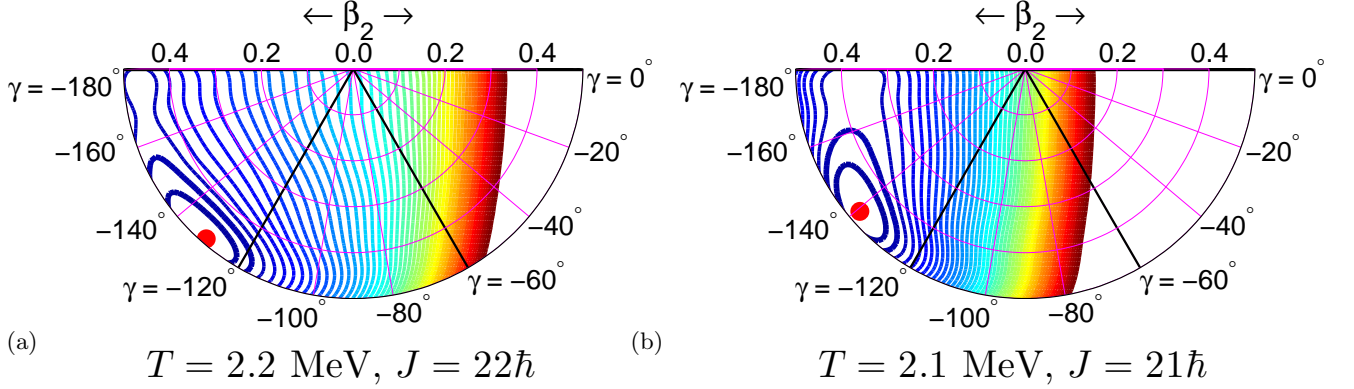


FIG. 3: (Color online) The free energy surfaces of (a) ^{31}P and (b) ^{28}Si for the measured T and J (contour line spacing is 0.2 MeV). Here, $\gamma = 0^\circ$ (-120°) represent the non-collective (collective) prolate shape and $\gamma = -180^\circ$ (-60°) represent the non-collective (collective) oblate shape. The most probable shape is represented by a filled circle.

Most noteworthy is the striking difference between the GDR spectra in two reactions leading to ^{31}P and ^{28}Si nuclei. Both ^{31}P and ^{28}Si , populated at the same initial excitation energy ($E^* \sim 70$ MeV) and with angular momentum $\langle J \rangle \sim 21 \hbar$ ($\pm 6 \hbar$). The J_C from systematics in Ref. [2] are $19 \hbar$ and $17 \hbar$ for ^{31}P and ^{28}Si , respectively. While ^{31}P spectrum shows the expected multicomponent character arising due to the Coriolis's splitting with a distinct low energy peak at ~ 9 MeV, the γ -ray spectrum of ^{28}Si does not show evidence of the Jacobi shape transition. It can be seen from the Fig. 1 that ^{28}Si yield shows significant enhancement at higher folds as compared to ^{31}P . Therefore, the measured fold distribution together with the fact that J_C is lower for ^{28}Si than that for ^{31}P , makes the non-occurrence of Jacobi shape transition in ^{28}Si very fascinating. Further, the γ -ray spectrum of ^{28}Si for $F \geq 6$ corresponding to $\langle J \rangle = 24 \hbar$ ($\pm 6 \hbar$) was also found to have same shape and no peak was visible around 10 MeV [see inset of Fig. 2(d)].

The measured GDR strength functions are compared with thermal shape fluctuation model (TSFM) calculations corresponding to the measured $\langle T \rangle$ and $\langle J \rangle$ values given in Table I. The details of the TSFM calculation are discussed in the Refs. [37–40], where shape fluctuations are treated by evaluating the expectation values of the observables (over the deformation degrees of freedom) with their probability given by the Boltzmann factor $\exp(-F/T)$. The free energy (F) is calculated within a microscopic-macroscopic approach by tuning the angular frequency to get the desired J . The calculated free energy surfaces (FES) are shown in Fig. 3, where it can be seen that the predicted equilibrium shapes for both ^{31}P and ^{28}Si are similar and both the nuclei are therefore expected to show similar behaviour -namely, the Jacobi shape transition. The calculated GDR cross-sections (σ_{TSFM}) are compared with the corresponding best fit statistical model calculation (σ_{stat}) in Fig. 4. Since the absolute cross-section is not measured in the present experiment, σ_{TSFM} was normalized to the total σ_{stat} in the energy region of $E_\gamma = 7 - 25$ MeV [41]. The variance in σ_{stat} is calculated from the errors of the best fit parameters. The ^{31}P data is in qualitative agreement with the TSFM predictions, but this is not the case for ^{28}Si . The TSFM predicts a low energy component (~ 10 MeV) for ^{28}Si , which is not corroborated by the data. Further, the TSFM calculations carried out without the shell effects are also shown in the same figure. It is seen that shell effects do not significantly affect the GDR cross-section at the measured T, J . The TSFM calculation does not include the pairing effect, which is expected to be negligible at $T \sim 2$ MeV. Therefore, it is evident that the GDR spectrum of ^{28}Si at high J is anomalous as compared to ^{31}P and this discrepancy can not be understood in terms of TSFM or microscopic factors like shell or pairing effects. It should be noted that $^{16}\text{O} + ^{12}\text{C}$ reaction has entrance channel isospin $T = 0$, which is expected to suppress the GDR yield [42] but is not expected to affect the shape of the GDR strength function.

Recently, similar observation- namely, the absence of Jacobi shape transition, was reported in ^{32}S populated via $^{20}\text{Ne} + ^{12}\text{C}$ reaction [23]. In both these cases (^{32}S and ^{28}Si), projectile-target involve self-conjugate α -cluster nuclei. As mentioned earlier, the reactions involving these nuclei are shown to exhibit orbiting phenomenon leading to formation of quasi-molecular states [19, 20]. The orbiting behaviour in $^{16}\text{O} + ^{12}\text{C}$ at $E_{lab} = 125$ MeV was reported earlier in charged particle studies [18]. In such molecular states, the configuration will have a two body rotor with mass concentrated on the periphery as opposed to a deformed nucleus with most of the mass at the center. Hence, the moment of inertia corresponding to a molecular resonance state is expected to be larger and consequently the angular frequency would be smaller. Thus, the formation of the dinuclear complex due to orbiting may suppress the Jacobi shape transition. Further, in case of quasi-molecular resonances there would be an interplay of rotational motion of the dinuclear complex and vibrational motion of constituent nuclei, which would result in the fragmented strength [43]. It should be pointed out that the net excitation energy as well as effective T and J for such a state can not

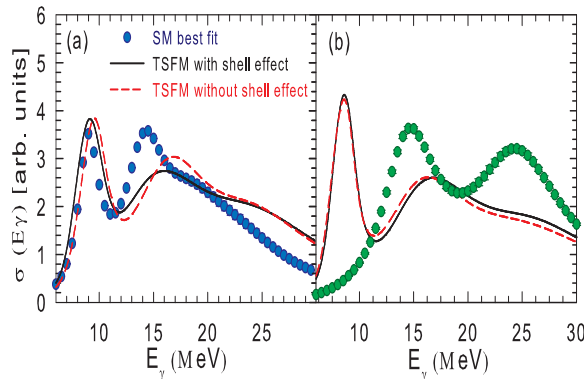


FIG. 4: (Color online) The best fit statistical model input cross-section (filled symbols) compared to TSFM calculations with (continuous line) and without (dashed line) Shell effect.

be estimated in a simple manner. Moreover, the statistical model analysis or TSFM, which assumes a formation of equilibrated CN, is not suitable to describe the data. Detailed theoretical calculations are required to understand whether the fragile correlations leading to molecular configurations survive thermal fluctuations. In addition, the role of possible binary shapes on GDR, at large excitations needs to be investigated. It is important to note that the ^{32}S GDR data [7, 23] has been analyzed only within the statistical model framework. However, deformations deduced for both ^{32}S , ^{28}Si from the conventional statistical model analysis are large ($\beta_2 > 0.6$) and point towards the elongated structure. It should be mentioned that the earlier data reporting the signature of orbiting in Ref. [36] from the charged particle spectra, have shown the co-existence of molecular resonance states with equilibrated compound nucleus formation. In such a scenario, it is possible that high J components of the entrance channel are predominantly contributing to the orbiting state and consequently the CN is formed with $J < J_C$. In the present experiment, γ -rays from CN with $\langle J \rangle \leq 15 \hbar$ (corresponding to $F < 3$) could not be unambiguously extracted.

In summary, the measurement of high energy γ -rays from the decay of giant dipole resonance in ^{31}P nucleus and a self-conjugate α -cluster nucleus ^{28}Si , populated at same initial excitation energy and $\langle J \rangle > J_C$ was carried out to study the Jacobi shape transition. The measured GDR spectrum in the decay of ^{31}P shows a distinct low energy component around 10 MeV, which is a clear signature of the Coriolis's splitting in a highly deformed rotating nucleus. This first observation of the Jacobi shape transition in ^{31}P , together with earlier results in $A \sim 40 - 50$ nuclei, show that Jacobi shape transition is a general feature of nuclei in light mass region. The observed GDR strength function in ^{31}P can be qualitatively explained by the TSFM. An anomalous behaviour is observed in the case of ^{28}Si , where the GDR lineshape can be explained as 2-components to a prolate deformed nucleus, and does not exhibit signature of Jacobi shape transition. Based on this data and similar recent results in ^{32}S , it is proposed that the nuclear orbiting phenomenon exhibited by α -cluster nuclei, hinders the Jacobi shape transition. The study of the GDR in self-conjugate α -cluster CN populated through different entrance channels comprising α -cluster and non- α cluster, would be important to understand the role of orbiting in nuclear structure. The present experimental results suggest a possibility to investigate the nuclear orbiting phenomenon using high energy γ -rays as a probe.

Acknowledgement

We would like to thank Mr. M.S. Pose, Mr. K.S. Divekar, Mr. M.E. Sawant, Mr. Abdul Quadir, Mr. R. Kujur for help with experimental setup, Mr. R.D. Turbhekar for target preparation and the PLF staff for the smooth operation of the accelerator. AKRK acknowledges the financial support from the DST-INSPIRE Faculty program (India) and RIKEN Supercomputer HOKUSAI GreatWave System for the numerical calculations. PA acknowledges financial support from the SERB (India), DST/INT/POL/P-09/2014.

-
- [1] R Beringer and W J Knox, Phys. Rev. 121 (1961) 1195.
 - [2] W. D. Meyers and W. J. Swiatecki, Acta. Phys. Pol. B 32 (2001) 1033.
 - [3] Mazurek et al., Phys. Rev. C 91 (2015) 034301.
 - [4] M. Kicińska-Habior et al., Phys. Lett. B. 308 (1993) 225.

- [5] A. Maj et al., Nucl. Phys. A 731 (2004) 319.
- [6] D. R. Chakrabarty et al., Phys. Rev. C 85 (2012) 044619.
- [7] Deepak Pandit et al., Phys. Rev. C 81 (2010) 061302R.
- [8] D. R. Chakrabarty, N. Dinh Dang and V. M. datar, Eur. Phys. J. A 52 (2016) 143.
- [9] D. Ward et al., Phys. Rev. C 66 (2002) 024317.
- [10] M. Freer, Rep. Prog. Phys. 70 (2007) 2149.
- [11] W. von Oertzen, M. Freer, and Y. Kanada-Enyo, Phys. Rep. 432 (2006) 43.
- [12] A. Shrivastava et al., Phys. Lett. B. 718 (2013) 931.
- [13] J. P. Ebran, E. Khan, T. Niksic and D. Vretenar, Nature 487 (2012) 341.
- [14] F. Hoyle, Astrophys. J. Suppl. Ser. 1 (1954) 121.
- [15] T. K. Rana et al., Phys. Rev. C 88 (2013) 021601R.
- [16] Martin Freer and H.O.U Fyndo, Prog. Part. Nucl. Phys. 78 (2014) 2149.
- [17] S. J. Sanders, A. Szanto de Toledo, and C. Beck, Phys. Rep. 311 (1999) 487.
- [18] S. Kundu et al., Phys. Rev. C 78 (2008) 044601.
- [19] Yasutaka Taniguchi et al., Phys. Rev. C 80 (2009) 044316.
- [20] T. Ichikawa, Y. Kanada-Enyo, and P. Moller, Phys. Rev. C 83 (2011) 054319.
- [21] C. Beck et al., AIP conference proceedings 1098 (2009) 207.
- [22] M.D. Salsac et al., Nucl. Phys. A 801 (2008) 1.
- [23] Deepak Pandit et al., Phys. Rev. C 95 (2017) 034301.
- [24] <http://www.tifr.res.in/~pell/lamps.html>
- [25] C. Ghosh et al., Phys. Rev. C 96 (2017) 014309.
- [26] D. R. Chakrabarty et al., Nucl. Instrum. Methods Phys. Res., Sect. A 560 (2006) 546.
- [27] C. M. Perey and F. G. Perey, At. Data Nucl. Data Tables 17 (1976) 1.
- [28] F. G. Perey, Phys. Rev. 131 (1963) 745.
- [29] L. Mcfadden and G. R. Satchler, Nucl. Phys. A 84 (1966) 177.
- [30] A. V. Ignatyuk, G. N. Smirenkin, and A. S. Tishin, Sov. J. Nucl. Phys. 21 (1975) 255 [Yad. Fiz. 21 (1975) 485].
- [31] Debasish Mondal et al., Phys. Lett. B. 763 (2016) 422.
- [32] D. R. Chakrabarty et al., Nucl. Phys. A 770 (2006) 126.
- [33] H. Nifennecker and J. A. Pinston, Annu. Rev. Nucl. Part. Sci. 40 (1990) 113.
- [34] K. Neegard et al., Phys. Lett. B. 110 (1982) 7.
- [35] D. R. Chakrabarty et al., J. Phys. G: Nucl. Part. Phys. 37 (2010) 055105.
- [36] S. Kundu et al., Phys. Rev. C 87 (2013) 024602.
- [37] P. Arumugam, G. Shanmugam and S. K. Patra., Phys. Rev. C 69 (2004) 054313.
- [38] A. K. Rhine Kumar, P. Arumugam and N. Dinh Dang., Phys. Rev. C 90 (2014) 044308.
- [39] A. K. Rhine Kumar, P. Arumugam and N. Dinh Dang., Phys. Rev. C 91 (2015) 044305.
- [40] A. K. Rhine Kumar and P. Arumugam., Phys. Rev. C 92 (2015) 044314.
- [41] C. Ghosh et al., Phys. Rev. C 94 (2016) 014318.
- [42] J. A. Behr et al., Phys. Rev. Lett. 70 (1993) 3201.
- [43] W. B. He, Y. G. Ma, X. G. Cao, X. Z. Cai and G. Q. Zhang, Phys. Rev. Lett. 112 (2014) 032506.